1

Is the Stratospheric QBO affected by Solar Wind Dynamic Pressure via an Annual Cycle Modulation?

Hua Lu[a,1], and Martin J. Jarvis[a]

Revised December 2010

---

[1]Corresponding author Email: hlu@bas.ac.uk
[a] Hua Lu, Martin. J. Jarvis, British Antarctic Survey, High Cross, Madingley Road, Cambridge CB3 0ET, United Kingdom. (email: hlu@bas.ac.uk; mjja@bas.ac.uk)

24

25   **Abstract:** In this study, statistical evidence of a possible modulation of the equatorial

26   stratospheric Quasi-biennial Oscillation (QBO) by the solar wind dynamic pressure is

27   provided. When solar wind dynamic pressure is high, the QBO at 30-70 hPa is found to be

28   preferably more easterly during July to October. These lower stratospheric easterly anomalies

29   are primarily linked to the high frequency component of solar wind dynamic pressure with

30   periods shorter than 3-years. In annually and seasonally aggregated daily averages, the

31   signature of solar wind dynamic pressure in the equatorial zonal wind is characterized by a

32   vertical three-cell anomaly pattern with westerly anomalies both in the troposphere and the

33   upper stratosphere and easterly anomalies in the lower stratosphere. This anomalous behavior

34   in tropical winds is accompanied by a downward propagation of positive temperature

35   anomalies from the upper stratosphere to the lower stratosphere over a period of a year. These

36   results suggest that the solar wind dynamic pressure exerts a seasonal change of the tropical

37   upwelling which results in a systemic modulation of the annual cycle in the lower

38   stratospheric temperature, which in turn affects the QBO during Austral late winter and

39   spring.

40

41

42

1. Introduction

The quasi-biennial oscillation (QBO) of the equatorial stratosphere is characterized by alternating easterly and westerly wind regimes and dominates the variability of the tropical lower stratosphere [*Naujokat*, 1986; *Baldwin et al*., 2001]. The winds descend from 10 hPa to 100 hPa at an averaging speed of 1 km/month and repeat at intervals from 18-36 months, with an average periodicity of ~28 months [*Pascoe et al*., 2005]. Our current understanding of the QBO is largely based on the theoretical augment of *Holton and Lindzen* [1972] who showed how vertically propagating equatorial waves are absorbed at a critical layer by the mean flow and in turn generate alternating acceleration of the zonal flow in either easterly or westerly directions [*Plumb and Bell*, 1982].

In addition to this wave-driven mechanism, seasonal or interannual variation of the QBO may also arise from seasonal changes in tropical upwelling [*Dunkerton*, 1991; 2000; *Holton et al*., 1995; *Kinnersley and Pawson*, 1996], shifting of latitudinal gradients in the subtropics [*Randel et al*., 1998], or variation of the semi-annual oscillation (SAO) in the tropical upper stratosphere [*Dunkerton and Delisi*, 1997]. Additional temperature change may be caused by the secondary circulation, induced by the QBO itself, which consists of an increase in the upwelling at the easterly shear zone and a suppression of the upwelling at the westerly shear zone [*Plumb and Bell*, 1982].

While the QBO is primarily driven by internal wave dynamics, a possible modulation of the QBO *via* external forcing cannot be ruled out. There is increasing evidence that part of variability in the stratosphere may be linked to the solar activity [*Haigh*, 2003; *Labiztke et al*., 2006; *Lockwood et al*., 2010; *Gray et al*., 2010]. Studies have indicated that solar variability may indirectly modulate the QBO through the variation in solar UV irradiance [*Salby and*

66   *Callaghan*, 2000; *Soukharev and Hood*, 2001; *McCormack*, 2003; *Mayr et al.*, 2005; 2006;

67   *McCormack et al.*, 2007]. Absorption of solar ultraviolet (UV) radiation by ozone may cause

68   changes in temperature and hence in the QBO near the equatorial stratosphere [*Hood*, 2004;

69   *Crooks and Gray*, 2005; *Pascoe et al.*, 2005]. Such anomalous heating in the upper

70   stratosphere may alter Rossby wave propagation and breaking [*Cordero and Nathan*, 2005;

71   *McCormack et al.*, 2007] and hence cause an indirect dynamic feedback through modulation

72   of the polar vortex and the Brewer-Dobson (BD) circulation [*Kodera and Kuroda*, 2002].

73   *Salby and Callaghan* [2000] examined the radiosonde equatorial zonal wind at 45 hPa for the

74   period of 1956−1996 and found that the average duration of the westerly QBO (wQBO)

75   around solar maxima is ~3−6 months shorter than that around solar minimum. *Soukharev and*

76   *Hood* [2001] performed composite analysis using the radiosonde-derived equatorial zonal

77   wind at 50 to 10 hPa from 1957 to 1999 and found that the duration of both QBO phases was

78   shorter at solar maxima than at solar minima. Using ECMWF ERA-40 reanalysis, *Pascoe et*

79   *al.* [2005] found that the average time required for the eQBO to descend from 15 hPa to 44

80   hPa is ~2 months less at solar maxima than at solar minima. By using a fully interactive 2D

81   Chemical/Dynamical Model, *McCormack* [2003] and *McCormack et al.* [2007] found that the

82   duration of the wQBO can be 1-3 months shorter at solar maximum than solar minimum.

83   They suggested that the ozone heating induced by solar UV in the upper stratosphere reduces

84   the tendency for a westerly wind and hence produces an anomalously stronger easterly wind

85   in the tropical upper stratosphere. By generating the QBO internally using a high resolution

86   general circulation model (GCM), *Palmer and Gray* [2005] showed that the durations of both

87   QBO phases may be reduced by up to 2 months at solar maximum. *Cordero and Nathan*

88   [2005] showed that prescribing higher solar UV inputs produces a QBO with shorter duration

89   and larger amplitude. In addition to the direct ozone heating, wave-ozone feedback has been

90   shown to modify the refraction of tropical quasi-stationary Rossby waves, reducing the

91   tropical upwelling and resulting in faster descent of eQBO [*Nathan and Cordero*, 2007].

92   *Mayr et al.* [2006] prescribed a synthetic period of 10-years with varying amplitude of

93   radiative forcing at three different heights (0.2% − surface, 2% − 50 km, 20% −100 km) and

94   their model simulation also resulted in a modulation of the QBO in the stratospheric

95   equatorial region which appeared to be generated by this synthetic SC modulation. *Mayr et*

96   *al.* [2005] suggested that an annual oscillation can originate near 60 km, through which the

97   prescribed 10-year modulation could be transferred downward and amplified by tapping the

98   momentum from the upward propagating gravity waves.

99   In contrast, other studies have been unable to find a significant link between solar UV

100   and QBO variability. *Hamilton* [2002] used data from 1950 to 2000 and found a quasi-

101   decadal variation in the duration length of the wQBO at 40-50 hPa but the connection with

102   the 11-year solar cycle noted by *Salby and Callaghan* [2000] did not always hold and the

103   correlation coefficient was only −0.1 when computed over a longer period which included 22

104   westerly phases. *Fischer and Tung* [2008] used radiosonde measurements for 1953-2005 and

105   showed that the correlations between the duration of the QBO and the 11-yr SC for either

106   phase of the QBO were close to zero. In addition, oppositely-signed correlations were found

107   to exist in the pre-1990 and post-1990 periods. More recently, *Kuai et al.* [2009] also dismiss

108   the solar cycle modulation of the QBO period. With exceedingly long model runs, those

109   authors found that a strong synchronization of the QBO period with integer multiples of the

110   Semi-Annual Oscillation (SAO) in the upper stratosphere may generate ''decadal'' variability

111   in the QBO period causing a waxing and waning of the correlation between solar forcing and

112   the QBO period. They therefore suggested that the SC-QBO duration relationship reported

113   previously reflects only a chance behaviour resulting from the use of relatively short

114   observational records.

115   In addition to solar UV, signature of the solar wind streaming out from the Sun has also

116   been found in various climate records [*Lu et al*., 2008a; *Lockwood et al*., 2010a,b; *Woollings*

117   *et al*., 2010]. The solar wind variability manifests itself at Earth in a number of ways but most

118   prominently through geomagnetic activity, thermospheric heating and the aurorae.

119   Observational studies have shown that the solar wind induced geomagnetic activity may alter

120   stratospheric chemistry indirectly through particle precipitation [*Solomon et al*. 1982; *Randall*

121   *et al*., 2005; 2007; *Seppälä et al*. 2007; *Siskind et al*., 2007]. Chemical-dynamical coupled

122   general circulation models (GCMs) have indicated that odd nitrogen (NO_x) induced by

123   energetic charged particle precipitation during geomagnetic storms may cause temperature

124   changes in both the polar and equatorial regions and in the stratosphere and the troposphere

125   [*Langematz et al*., 2005; *Rozanov et al.,* 2005; *Seppälä et al*. 2009].

126   Other studies suggested that solar wind induced geomagnetic activity may perturb

127   atmospheric circulation through a change in planetary wave reflection conditions [*Arnold and*

128   *Robinson*, 2001; *Lu et al*. 2008b]. Model simulations by *Arnold and Robinson* [2001] have

129   indicated that a change in planetary wave reflection conditions at the lower thermospheric

130   boundary caused by thermsopheric heating induced by solar wind driven geomagnetic

131   activity can reduce planetary wave propagation into the stratosphere, leading to a

132   strengthening of the stratospheric polar vortex and a weakening of the BD-circulation.

133   Significant correlations have also been established between geomagnetic activity and lower

134   stratospheric temperature by *Lu et al*. [2007]. They found that the temperature response to

135   the 11-yr SC and geomagnetic Ap index tend to enhance each other in the tropical upper

136   troposphere and lower stratosphere, the magnitude of the response to geomagnetic activity

137   being slightly larger than that associated with the 11-yr SC. *de Artigasa and Elias* [2005]

138   have shown that, when solar flux is high, the eQBO (at 15-50 hPa) is more likely to be

139   associated with high geomagnetic activity and the wQBO is more likely to be associated with

140   low geomagnetic activity; at solar minimum, this relationship is reversed. *Lu et al*. [2008a]

141   have shown that there is a robust relationship between solar wind dynamic pressure and the

142   zonal wind and temperature in the northern polar winter. Stratospheric wind and temperature

143   variations are positively projected onto the Northern Annular Mode (NAM) when the 11-yr

144   SC is at its maximum phase, and negatively projected onto the NAM during the 11-yr SC

145   minimum phase. This implies a weakening of the BD-circulation with reduced upwelling into

146   the lower stratosphere at low-latitude under high solar wind forcing, consistent with the

147   tropical warming signals detected by *Lu et al.* [2007].

148   While variations in solar radiation are most strongly seen in the 11-year solar cycle, the

149   solar wind induced geomagnetic activity exhibits a strong variability at shorter time scales.

150   *Lu et al*. [2008a] shows that the solar wind dynamic pressure and F10.7 solar flux are poorly

151   correlated, largely due to those shorter time variations. Their weak statistical dependence

152   allows the signals associated with the 11-year solar irradiance and the solar wind dynamic

153   pressure to be separated. However, their mechanisms may not be mutually exclusive and they

154   could be acting together to either enhance or cancel the overall atmospheric responses.

155   Motivated by these results and rather strong extra-tropical signals in NH winter and

156   spring observed by *Lu et al*. [2008a], a statistical analysis is conducted here to study possible

157   solar wind dynamic pressure perturbations near the tropics, with a primary focus on detecting

158   possible solar wind perturbation of the QBO. We use solar wind dynamic pressure, instead of

159   geomagnetic indices, because geomagnetic indices are measured through the interaction of

160   the terrestrial environment with the solar wind and are therefore not completely independent

161   of internal Earth atmospheric processes. For instance, *Sugiura and Poros* [1977] identified a

162   QBO-like periodicity in the disturbed storm time current (Dst) and hence in geomagnetic

163   activity, and *Jarvis* [1996] has shown a QBO periodicity in geomagnetic daily range induced

164   by the semidiurnal tide. Conversely, the solar wind dynamic pressure is measured well

165 outside of Earth's magnetosphere and is therefore wholly independent to the internal

166 variability of the Earth's atmosphere. Nevertheless, it can be shown that similar but slightly

167 weaker results are obtainable by using geomagnetic *Ap* index.

2. Data and Methods

169 In this study, daily QBO is defined as the deseasonalized daily zonal-mean zonal wind

170 averaged over the latitude band of 5°S-5°N for five pressure levels at 70, 50, 30 20 and 10

171 hPa. Zonal-mean zonal winds are extracted from the ECMWF (European Centre for Medium

172 Range Weather Forecasting) ERA40 Reanalysis (September 1957 to August 2002) and

173 ECMWF Operational analyses (September 2002 to December 2009). The ERA-40 Reanalysis

174 was assimilated using direct radiosonde and satellite measurements [*Uppala et al.*, 2005]. It

175 has a spectral resolution of T159, corresponding to a 1.125º horizontal resolution in latitude

176 and longitude and are available at 23 standard pressure surfaces from 1000 hPa to 1 hPa. The

177 ECMWF Operational data were output from the ongoing analyses produced by the most

178 recent ECMWF Integrated Forecasting System (IFS) model. Data from September 2002 to

179 the present day are available on the same 1.125º grid and but on 21 pressure levels (before

180 07/11/2007) and 25 pressure levels (since 07/11/2007). The ERA-40 and the Operational data

181 sets share 21 pressure levels; the exceptions are four levels in the lower troposphere (*i.e*. 600,

182 775, 900, and 950 hPa) which are excluded from this analysis. Nevertheless, the two data sets

183 share the same five pressure heights where the QBOs are estimated.

184 It has been established that before the satellite era (*i.e*. before September 1978), the

185 scarcity of SH radiosonde measurements and lack of direct measurement at altitudes above

186 10 hPa resulted in unreliable estimations in ERA-40, particularly in the southern hemisphere

187 and in the upper stratosphere. In the tropics, however, *Baldwin and Gray* [2005] showed that

188 the QBO extracted from ERA-40 is consistent with rocketsonde winds (that were not

189   assimilated by ERA-40) measured at Ascension and Kwajalein up to the 2-3 hPa altitude

190   level, even for those years before the satellite era. *Pascoe et al.* [2005] also found that the

191   ERA-40 accurately describes the QBO and the tropical stratospheric circulation. We also

192   compared the monthly averaged QBO with those available at the Free University of Berlin

193   (FUB) [*Naujokat*, 1986] for the five pressure levels used here. The two data sets are in good

194   agreement with a correlation coefficient greater than 0.9 for all five pressure levels. In

195   addition, the response to solar wind dynamic pressure reported in this paper is found

196   primarily below 10 hPa. Hence, for these reasons, the results reported here make use of all

197   available data since 1963. Figure 1 shows latitudinally integrated zonal-mean zonal wind at

198   5°S-5°N as a function of height (1-100 hPa) for the period of 1958-2009.

199   **[insert figure 1 here]**

200   The upper two panels of figure 1 display the original monthly mean data while the lower

201   two panels show its deseasonalized anomalies. A prominent Semi-Annual Oscillation (SAO)

202   exists near the stratopause level when the data is not deseasonalized. Once deseasonalization

203   is applied, the descending alternating easterly and westerly winds of the QBO are the

204   dominant feature, with maximum amplitude of ~40 m s^{-1} at ~3-5 hPa, where the QBO is

205   initialized. In the upper stratosphere, discernible enhancement of easterly anomalies occurred

206   in the 1970s while an enhancement of westerly anomalies occurred from the mid- 1980s to

207   the late 1990s. From 2000 onwards, it becomes comparable to the earlier pattern again. It has

208   been suggested that the enhanced westerly anomalies seen in the upper stratosphere during

209   the 1980s and 1990s might be a result of data assimilation pre-/post- satellite era [*Punge and*

210   *Giorgetta*, 2007]. The extended data seem to suggest it is more likely to be a real

211   phenomenon in which a multi-decadal variation is superimposed upon the upper stratospheric

212   SAO.

213   Solar wind dynamic pressure (P_{sw}) measured in Geocentric Earth Magnetic (GEM)

214   coordinates is obtained from the NASA-OMNI site (http://omniweb.gsfc.nasa.gov/). This

215   data set is produced from solar wind and interplanetary magnetic field measurements from 15

216   geocentric satellites and 3 spacecraft in orbit around the L1 Sun-Earth Lagrange point and has

217   been carefully compiled through cross-calibration. P_{sw} has been calculated by NASA-OMNI

218   as $P_{sw} = 1.6726 \times 10^{-6} N_{sw} V_{sw}^2$, where N_{sw} is the flow density in number of particles per cm^3

219   and V_{sw} is the solar wind speed in km s^{-1}. In physical terms, P_{sw} represents the momentum

220   flux of the solar wind and has a unit of nPa (nano Pascals). Daily averages of solar wind P_{sw}

221   from January 1963 to December 2009, covering ~4.5 solar cycles, together with its monthly

222   mean are used here. The main advantage of using the daily data over the monthly mean is that

223   the downward decent of the signals can be studied in more detail.

224   There are a few missing data periods of P_{sw} due to inappropriate positioning of satellites

225   or instrument failure. For instance, before August 1965, and also between September 1982

226   and October 1994, the data availability is below 50% at hourly resolution, with 8–15

227   complete days showing as missing data in each month [*King and Papitashvili*, 2005]. For up

228   to 3 days of missing values, a simple interpolation is used to fill the gap. For longer missing

229   data periods, no treatment is applied and those days are ignored by the analysis. For the

230   months with more than 15 day missing values, monthly P_{sw} is treated as missing data. The

231   effect of missing data for running composite/regression is that different months or seasons

232   under investigation may involve different sample lengths. While the monthly P_{sw} varies from

233   1.2 to 6.7, the daily P_{sw} varies from 0.1 to 27 nPa with an arithmetic mean value of 2.5 nPa

234   and standard deviation of 1.5 nPa (not shown).

235   Figure 2 shows monthly mean P_{sw} and its high and low frequency components, where the

236   separation cutoff period is 36-month. The low frequency P_{sw} shows a quasi-decadal variation

237   superimposed on a slow varying trend. Its quasi-decadal variation peaks at the minimum

238   phase of the 11-year solar cycle suggesting an 11-year solar cycle modulation on P_{sw}. There

239   is clear evidence of slow-varying 11-year cycle in its high frequency component.

240   Nevertheless, over the period 1963-2009, the correlation coefficient between P_{sw} and sunspot

241   number or F10.7 solar flux is below 0.1 on a daily timescale and remains below 0.2 for the

242   monthly mean. This is largely due to the high frequency variation of P_{sw}. Thus, any

243   significant $P_{sw,}$ signals especially those associated with its high frequency component, should

244   be fairly statistically independent to the signature associated with the 11-year solar cycle.

245   **[Insert figure 2 here]**

246   For simplicity, we use $\bar{P}_{sw} < -0.25$ and $\bar{P}_{sw} > 0.25$ to define low and high solar wind

247   dynamic pressure either for the raw P_{sw} or its high frequency component, where $\bar{P}_{sw}$ stands

248   for the median-normalized values of P_{sw}; transition periods where $|\bar{P}_{sw}| \leq 0.25$ are excluded.

249   The same rule is applied to differentiate the westerly and easterly QBO phases. Qualitatively

250   similar results can be obtained if other definitions, such as mean instead of median for $\bar{P}_{sw}$,

251   are used. Hereinafter, high and low solar wind dynamic pressure are abbreviated as HP and

252   LP.

253 # 3.   Results

254   *3.1   Perturbations caused by Solar Wind Dynamic Pressure*

255   Figure 3 shows the QBO phase occurrence by month as a percentage separated into high

256   (upper panel) and low (lower panel) solar wind dynamic pressure for 70hPa (left), 50 hPa

257   (central) and 30hPa (right) estimated using daily data. Under HP, the difference in occurrence

258   between eQBO and wQBO is noticeably smaller than it is under LP at all three pressure

259   levels and the difference even reverses at 30 hPa. The largest difference occurs under LP

260   conditions during the Austral winter and spring and reduces with increasing altitude. The

261   departure between the QBO phase occurrence under HP and LP begins in June to July. By

262   assuming that both the QBO and P_{sw} follow a first-order auto-regressive (AR1) process, we

263   use a Monte Carlo trial-based test [*Wang et al.*, 2006] to determine the significance of the

264   differences. It is found that the differences under LP at 50 hPa and 70 hPa are significant at

265   the 95% confidence level only for July to October while the difference at 30 hPa are

266   significant at the 95% for almost the entire year (except December and January). As a whole,

267   the behavior of the QBO phase occurrence differs from January to June, when the occurrence

268   of wQBO hardly changes from LP to HP, to July to December when the occurrence of

269   wQBO increases and the occurrence of eQBO decreases significantly under LP. This

270   suggests a higher eQBO to wQBO occurrence ratio in the lower stratosphere under HP than

271   under LP conditions. It suggests that under HP conditions there is either anomalously more

272   eQBO descent down from higher altitudes or a slower descent rate of the eQBO at 30-70 hPa.

273   The difference becomes weaker and not significant at higher altitudes.

274   **[Insert Figure 3 here]**

275   The same conclusion can be reached if the QBO phase occurrence is grouped according

276   to QBO phase and then the occurrence percentages calculated for HP and LP conditions (see

277   figure 4). At 70 hPa during September, nearly 50% of eQBO occurrence takes place under

278   HP compared with only 20% under LP; the difference becomes considerably smaller for

279   wQBO. The differences under eQBO for August-October for the all three pressure levels

280   from 30 to 70 hPa are significant at the 95% confidence level or above and at the 90%

281   confidence level for July. This confirms that significantly more eQBO occurred in the lower

282   stratosphere during the Austral late winter and spring and a positive relationship exists

283   between P_{sw} and increased eQBO occurrence.

284   **[Insert Figure 4 here]**

285   Figure 5a shows the vertical profile of annual mean equatorial zonal wind (solid line) plus

286   and minus its one standard deviation. Greater variability exists in the stratosphere than in the

287   troposphere largely due to the QBO. Figure 5b;c;d shows the vertical profile of tropical zonal

288   wind anomalies for separated HP and LP conditions under three different sampling

289   conditions, *i.e.* for (b) for 1963-2009, (c) for 1979-2009 and (d) for 1963-2009 but with

290   volcanic eruption affected data excluded. All the vertical profiles of zonal wind anomalies are

291   calculated by using daily deviation from its long-term mean and then aggregating to its

292   annual average. It shows that the modulation of solar wind dynamic pressure on daily

293   equatorial zonal wind is marked by a vertically 3-cell structure with westerly anomalies

294   ($\sim$0.3-0.5 m s^{-1}) in the troposphere, easterly anomalies ($\sim$2 m s^{-1}) at 20-70 hPa and westerly

295   anomalies ($\sim$3 m s^{-1}) at 3-10 hPa under HP-LP. As a whole, this vertical structure accounts

296   for $\sim$5-10% of one standard deviation of the tropical zonal wind for each associated vertical

297   region and these wind differences are significant at the 95% confidence level. Changing the

298   data period from 1963-2009 (figure 5b) to 1979-2009 (figure 5c) or excluding the years

299   affected by major volcanic eruptions (figure 5d) does not alter its general pattern or

300   significant levels. Similar results can also be obtained by excluding the years affected by the

301   major Niño events.

302   **[Insert Figure 5 here]**

303   Figure 6 shows that the same vertical profile of equatorial zonal wind anomalies also

304   holds on a seasonal time scale and the general vertical structure remains across all four

305   seasons (*i.e.* December-February, March-May, June-August, and September-November). In

306   the lower stratosphere, the largest and most significant departure from zero wind occurs

307   during Austral winter (June-August). A closer examination also suggests that there is a

308   noticeable seasonal variation in its vertical structure. From December to February, an upward

309   shift is obtained for the bottom cell of the stratosphere; from September to November, a

310   downward shift is apparent for both top and bottom cells in the stratosphere. The largest

311   differences between HP and LP conditions in the upper stratosphere occur in SON and DJF

312   while in the lower stratosphere they occur in MAM and JJA. Similar results can also be

313   obtained by excluding the years affected by either the major Niño events or the major

314   Volcanic eruptions.

315   **[Insert Figure 6 here]**

316   Figure 7a shows the 31-day running composite difference (HP − LP) of the equatorial

317   zonal mean zonal wind from June to October. Significant easterly anomalies (~8 m s^{-1}) are

318   found in 30-70 hPa pressure levels while westerly anomalies (~1 m s^{-1}) are simultaneously

319   detected in the upper troposphere. It is apparent that the stratospheric easterly anomalies

320   descend from 10 hPa or above from June and become significant from late July to early

321   October. Figure 7b shows the same running composite difference except that a high pass

322   filter with a cut-off period of 1095-days (~3 years) is applied to the daily P_{sw}. Note that both

323   the strength of the composite difference and the statistical confidence level are enhanced in

324   the stratosphere, suggesting that not the decadal-scale variability of P_{sw} but the variation of

325   P_{sw} at periods below 3 years is responsible for the easterly anomalies at 30-50 hPa. Longer

326   term variation of P_{sw} appears to be responsible to the anomalies at and below 70 hPa.

327   **[Insert Figure 7 here]**

328   The radiative heating induced by volcanic aerosols may also influence the lower

329   stratospheric temperature which in turn may lead to stalling of the downward propagation of

330   the QBO [*Dunkerton*, 1983]. To examine possible contamination by the temporary heating

331   caused by volcanic aerosols, Figure 7c shows the same composite difference as Figure 7b but

332   with the major volcanic affected data (*i.e.* Agung in March, 1963, El Chichón in March,

333   1982, and Pinatubo in June, 1991) excluded. A quantitatively similar result is obtained,

334   suggesting that those easterly anomalies in the lower stratosphere are not strongly biased by

335   the major volcanic induced warming in the lower stratosphere. Note that there are quite a lot

336   of missing data in the daily P_{sw} during 1963, 1964, 1982 and 1983 (see figure 2), the

337   contamination of those years are already excluded in the analysis of figure 7a;b, meaning that

338   the data affected by Pinatubo volcanic eruptions are the only difference between figure 7b

339   and 7c.

340   It has been observed that ozone concentrations and temperature in the tropical lower

341   stratosphere (~70 hPa) are anomalously low during the El Niño phase of the El Nino –

342   Southern Oscillation (ENSO) [*Randel et al.*, 2009]. To examine possible bias due to the large

343   cooling effect caused by the major El Niño events, figure 7d shows the same analysis as

344   figure 7b but with the major El Niño (*i.e.* 1972, 1973, 1982, 1983, 1997, and 1998) affected

345   years excluded. Note that, due to missing P_{sw} in 1982 and 1983, the data affected by 1972,

346   1973, 1997 and 1998 represent the only difference between figure 7b and 7d. Again a

347   quantitatively similar result is obtained, suggesting that the major El Niño events do not alter

348   the QBO- P_{sw} relationship significantly.

349   Figure 8 summarizes the effect of the higher frequency (< 3-yrs, the red line in figure 2)

350   components of P_{sw} on the QBO at 50 hPa and 30 hPa (figure 8a;d), where both P_{sw} and the

351   QBO are averaged from July to October. These pressure levels and months are chosen

352   because the results shown in figures 3, 4 and 7 suggest the largest effect of P_{sw} on the QBO at

353   those levels and during those months. At both pressure levels, there are significant negative

354   correlations between mean P_{sw} and the mean QBO. Neither Volcanic eruption nor El Niño

355   affected years are found to dominate or alter the correlations significantly. This helps to rule

356   out a possible linear contamination of the QBO- P_{sw} relationship by volcanic eruption and the

357   major El Niño events. However, it does not rule out the possibility that the ENSO might

358   modulate the QBO- P_{sw} relationship through non-linear processes and a possibility

359   modulation in other calendar months or at different frequency. This is beyond the scope of

360   the current study.

361   **[Insert Figure 8 here]**

362   Figure 9 shows the running composite HP – LP difference of the equatorial zonal mean

363   temperature from January to December. The largest positive anomalies (~2 K) are found from

364   August to November at 30-50 hPa. Positive anomalies (~ 1 K) are also found at 70-150 hPa

365   (becoming significant between 100 and 150 hPa) during the December to June period while

366   significant negative anomalies (~ 0.5 K) are detected at 300-700 hPa between July and

367   October. The two most striking and significant features of figure 9 are: 1) downward

368   propagation of positive temperature anomalies in the upper stratosphere from December of

369   the previous year to the lower stratosphere in December of the following year; 2) the

370   anomalous warming at ~100 hPa during the Boreal winter and spring and anomalous cooling

371   at 700-300 hPa during the Austral winter. The combined effect of these temperature

372   anomalies is a systematic annual modulation of the annual oscillation of temperature in the

373   lower stratosphere related to solar wind dynamic pressure.

374   **[Insert Figure 9 here]**

375   Such annual cycle modulation can be compared to the annual oscillation normally

376   present in the stratosphere. Figure 10a shows the climatological mean annual pattern of the

377   tropical zonal mean zonal wind. The strongest variation appears in the upper stratosphere (1-5

378   hPa) with a semi-annual cycle clearly visible. In the lower stratosphere (50-100 hPa), a

379   weaker semi-annual cycle also exists and this is roughly in phase of that in the upper

380   stratosphere. In addition, there is a pronounced annual cycle both in the upper and lower

381   stratospheres. In the upper stratosphere, the annual cycle is marked by nearly 3 times stronger

382   easterly winds in the Boreal winter (~40 m s^{-1}) than in the Austral winter (~15 m s^{-1}). In the

383   lower stratosphere, the situation reverses with weaker easterlies occurring in the Boreal

384   winter (~2 m s^{-1}) and stronger easterlies in the Austral winter (~5 m s^{-1}). In the 10-50 hPa

385   region where the QBO prevails, the magnitude of zonal mean wind is primarily easterly (~15

386   m s^{-1}). It also shows a modulation by an annual cycle, albeit weak, with stronger easterly

387   winds occurring in the Austral winter.

388   **[Insert Figure 10 here]**

389   Figure 10b shows the temperature anomaly (shaded contours) compared to the

390   climatological altitude dependent mean value of tropical zonal mean temperature (thick solid

391   lines). In the upper stratosphere, similar to the winds, the SAO dominates. The amplitude of

392   temperature there during the Boreal winter and spring (4-5 K) is about twice as large as it is

393   in Austral winter and spring (2-3 K), implying an additional annual cycle influence. An

394   annual cycle dominates at 50-100 hPa with a magnitude of −3 K during the Boreal winter and

395   4 K in Austral winter, a peak-to-peak value of ~8 K at 70 hPa. The semi-annual cycle in the

396   upper and the annual cycle in the lower stratosphere oppose each other during the Austral

397   winter, resulting in a close to flat temperature climatology at ~20 hPa. The climatological

398   tropical mean wind and temperature compare well with previously studies [*Baldwin et al.*,

399   2001; *Pascoe et al.*, 2005; *Fueglistaler et al.*, 2009].

400   Thus the annual oscillation linked to solar wind dynamic pressure (figure 9) works in

401   opposition to the normal annual oscillation in the lower stratosphere (*i.e.* 50-100 hPa),

402   reducing its amplitude. It is possible that, because the eQBO is most sensitive to diabatic

403   change in the lower stratosphere and particularly to temperature changes near the tropopause

404   [*Kinnersley and Pawson*, 1996], the modulation effect of solar wind dynamic pressure is

405   stronger for eQBO than for wQBO.

406   The seasonal variations of the equatorial wind and temperature anomalies in relation to

407   the variation of solar wind dynamic pressure can also be compared with the seasonal statistics

408   of QBO phase transitions. Figure 11 shows every major phase transition of the QBO between

                                                                                              17

409   1953 and 2009 at five different pressure levels grouped by months into histograms, where the

410   transitions before 1958 were determined by using deseasonalized monthly radiosonde data

411   and after 1958 were based daily data. The months where the transitions occurred may differ

412   by a month or two when compared to the earlier findings [*Dunkerton*, 1990; *Baldwin et al.*,

413   2001; *Hampson and Haynes*, 2004; *Christiansen*, 2010] as our deseasonalization is based on

414   extended daily (instead of monthly) data from 1958-2009. In terms of the general

415   distribution of the transitions, they remain similar to the previous studies based on radiosonde

416   estimates, especially at 50 hPa. At 30 hPa, the peak of the phase transition tends to occur

417   about two months earlier than those based on monthly NCEP reanalysis [see fig. 1 of

418   *Hampson and Haynes*, 2004].

419   The histograms of transitions at 30-70 hPa show a noticeable annual cycle variation for

420   both QBO phases. It is clear from Figure 11 that at 30 and 50hPa the transitions occur less

421   often from July to November than other months. The months and pressure levels with

422   reduced QBO phase transition coincide with the period/the height when/where the effect of

423   solar wind dynamic pressure on both equatorial zonal wind and temperature is most

424   significant (see figures 9 and 7). Similarly, the transitions of both the QBO phases at 10 hPa

425   occurred far less often during NH winter and spring than during other months. Again, this

426   coincides with the period when solar wind dynamic pressure related positive temperature

427   anomalies were found to be present at that pressure level and above (see figure 9).

428   **[Insert Figure 11 here]**

429   # 4. Discussions

430   The variability of the stratospheric QBO is known to be largely characterized by the

431   "stalling" of easterly QBO (eQBO) near 30 to 50 hPa as the easterly shear zone tends to

432   descend more irregularly than the westerly shear zone [*Naujokat*, 1986]. Modeling

433 simulations have suggested that the "stalling" of the QBO depends critically on whether

434 deposition of easterly momentum at the equator is sufficient to overcome the tendency for the

435 easterly shear zone to be advected upward or held static by the combination of the BD-

436 circulation and the QBO-induced residual circulation [*Dunkerton*, 1991; 2000; *Kinnersley*

437 *and Pawson*, 1996]. The tropical upwelling of the BD-circulation acts to slow down the

438 descent rate of the QBO and consequently extends the QBO period, or increases the

439 occurrence frequency for a given QBO phase. Because of the QBO-induced residual

440 circulation, the effect of the tropical upwelling on the descent of the shear zone depends on

441 the QBO phase. Upward motion is associated with eQBO [*Plumb and Bell*, 1982]: it

442 strengthens the upwelling so that the descent of the easterly shear zone is slowed further.

443 Conversely, downward motion is associated with wQBO: it causes cancellation of the

444 tropical upwelling so that the BD-circulation imposes a smaller slowing effect on the descent

445 of westerly shear zone. As a whole, the descent rate of the wQBO is less affected by

446 variations associated with the BD-circulation than that of the eQBO [*Kinnersley and Pawson*,

447 1996; *Dunkerton*, 2000; *Hampson and Haynes*, 2004].

448 The annual variation of the QBO may arise from a seasonal variation of the BD-

449 circulation, which is explained by the ''extratropical stratospheric pump'' mechanism

450 [*Holton et al.*, 1995]. This is dynamically driven by momentum dissipation of extratropical

451 waves so that air is drawn upward from the tropical troposphere and then poleward and

452 downward at high latitudes causing a seasonal variation in the BD circulation [*Yulaeva et al.*,

453 1994]. The periods with stronger overturning require stronger diabatic heating at the

454 ascending branch and cooling at the descending branch, which cools the stratosphere in the

455 tropics and warms it in the polar region. Because the planetary wave drag in the stratosphere

456 is stronger in the northern hemisphere (NH) winter than in the southern hemisphere (SH)

457 winter, it drives stronger upwelling and lower temperatures in the tropical lower stratosphere

458   during NH winter. As a result, the descent of the eQBO is preferentially stronger during the

459   months of May to July, when the tropical upwelling in the lower stratosphere is weakest

460   [*Baldwin et al.*, 2001]. Here we show that, on top of the modulation due to the extratropical

461   wave-driven BD-circulation, solar wind dynamic pressure may also perturb the tropical zonal

462   wind in the lower stratosphere and the largest effect is detected during July to October.

463   It is known that the annual cycle in lower stratospheric temperature plays an important

464   role in the QBO phase transition and occurrence [*Fueglistaler et al.*, 2009]. Previous studies

465   have suggested that the annual synchronization of the QBO phase transition is linked to

466   seasonally varying tropical upwelling [*Dunkerton*, 1990; *Hampson and Haynes* 2004] and the

467   annual cycle is a consequence of faster (slower) tropical upwelling in the Boreal (Austral)

468   winter [*Yulaeva et al.*, 1994; *Holton et al.*, 1995; *Rosenlof*, 1995]. More recent studies have

469   however challenged the "extratropical pump mechanism" and have resulted in some debate

470   regarding the processes driving upwelling in the tropical BD branch [*Fueglistaler et al.*,

471   2009]. It has been shown by both observation and numerical calculation that tropical wave

472   forcing produced by convective motion may also be partially responsible for the variation in

473   the lower stratospheric temperature and the QBO [*Norton*, 2006; *Randel et al.*, 2008*; Lu et*

474   *al.*, 2009; *Taguchi*, 2009]. Here, we present some statistical evidence of a possible

475   modulation of the lower stratospheric annual cycle via solar wind dynamic pressure P_{sw} and

476   the descent pattern of the QBO and tropical temperature anomalies. We show that there is a

477   significant perturbation of tropical zonal wind, apparently related to P_{sw}, in both the

478   stratosphere and the troposphere. Based on these results, we suggest that, in addition to

479   atmospheric internal variability, solar wind driven modulation may also play a role in causing

480   inter-annual variation in the strength and descent pattern of the QBO.

481   More recently, *Lu et al*. [2009] found that the processes that synchronize the QBO exert

482   different effects on different QBO phases from season to season. During July and August, the

483 phase speed is significantly slowed when westerlies prevail through the pressure levels, and

484 becomes more irregular when easterlies are dominating there. They found that tropical

485 upwelling alone is insufficient to explain the more irregular behaviour of the eQBO shear

486 zone during SH winter and suggested that changes in tropical waves could be involved. A

487 possible modulation of the QBO by solar wind dynamic pressure may provide a partial

488 explanation for their observation. Our results on solar wind dynamic pressure related

489 perturbation of the QBO add another element to this general picture of the QBO variability

490 mechanisms. As tropical upwelling is generally lower during the Austral winter and spring, a

491 seasonal temperature perturbation linked to high P_{sw} may create an environment which

492 favours significantly more easterly shear zone to descend from higher altitudes into the lower

493 stratosphere, and/or a slower descent of the QBO overall.

494   It is worth noting that the seasonal temperature change that we find to be related to solar

495 wind dynamic pressure in the stratosphere is ~1 K in the lower stratosphere and ~2 K in the

496 upper stratosphere. These values are comparable to the inter-annual variability of tropical

497 temperature associated with ENSO, volcanic eruptions, and the QBO [*Randel et al.*, 2004;

498 *Fueglistaler et al.*, 2009].

499   Our analysis of including or excluding the data affected by the major Volcanic eruptions

500 or the major El Niño events showed no obvious bias on the statistically significant

501 modulation of P_{sw} on the QBO. Nevertheless, more detailed study is needed to separate the

502 effects of Volcano, ENSO, solar UV and solar wind. One obvious method is multivariate

503 regression. However, the main drawback of such analysis is that these mechanisms may not

504 be mutually exclusive and they could act together in a non-linear fashion to either enhance or

505 cancel the overall responses. In addition, multivariate regression effectively reduces the

506 degree of the freedom in the data and results in statistically less significant results. Thus, it

507 remains technically challenging to separate the different origin/cause based on limited

508   observational data, especially when the interaction is non-linear between the regressive

509   variables.

510   *Lu et al*. [2008a] showed that the winter Northern Annular Mode (NAM) is positively

511   correlated with P_{sw} when the 11-yr SC is at its maximum phase while negative correlation

512   between P_{sw} and the stratospheric NAM exists in spring at solar minimum. Those

513   extratropical signals suggested a weakening of the BD-circulation during winter months with

514   reduced upwelling in the low-latitude lower stratosphere when both solar activity and solar

515   wind dynamic pressure are high. The reversed relationship in spring implies enhanced BD-

516   circulation and anomalous stronger upwelling at low latitudes. Our findings here (see figure

517   9) further confirm a seasonal modulation of the BD-circulation, reflected by a significant

518   increase of tropical lower stratospheric temperature which corresponds to an anomalously

519   weaker upwelling near the tropics. . It is also consistent with earlier findings of *Lu et al*.

520   [2007] based on geomagnetic Ap index.

521   It should be noted that distinct differences exist in the extratropical and tropical

522   responses. Firstly, the tropical response reported here does not change sign between winter

523   and spring as opposed to the P_{sw} projection onto the NAM which tends to switch from

524   positive to negative from NH winter to spring [*Lu et al*., 2008a]. Secondly, the tropical P_{sw}

525   signals are independent of the 11-yr SC while conversely the extratopical signals are only

526   statistically significant once the data are separated into high and low solar activity. Finally, a

527   significant response of the QBO to the P_{sw} variation is detected during SH late winter and

528   spring rather than during NH winter, when the most robust P_{sw} versus NAM relationship

529   holds. Hence, there is no clear evidence to suggest that the tropical response is a direct result

530   of the NH extra-tropical response reported previously by *Lu et al*. [2008a]. This implies that a

531   change in extratropical wave forcing alone is insufficient to explain the signals observed in

532   both the NH polar region during the Boreal winter and spring and the equatorial region

533　　during the Austral winter and spring. There must be either extra or different mechanisms at

534　　play to cause the incompatible signals in the extratropical NH winter.

535 **5. Summary**

536　　　　By using daily and monthly data extending from 1963 to 2009, we have revealed a

537　　significant solar wind dynamics pressure (P_{sw}) relationship to the annual cycle of temperature

538　　in the tropical tropopause region, which in turn affects the QBO during Austral late winter

539　　and spring. The main characteristics of this relationship can be summarized as follows.

540　　　1)　A significant change in both the strength and phase occurrence frequency of the QBO

541　　　　　in the lower stratosphere are found in the lower stratosphere in relation to the solar

542　　　　　wind dynamic pressure. The signature is manifested by stronger and more frequent

543　　　　　occurrence of easterly anomalies associated with high P_{sw} during July-October in the

544　　　　　lower stratosphere. The effect is related to much higher frequency variations of P_{sw}

545　　　　　than the 11-year solar cycle and the most significant response is found at 30-50 hPa.

546　　　2)　The annual averaged vertical profile of the tropical zonal wind anomalies caused by

547　　　　　P_{sw} perturbation is characterized by a vertical three-cell anomaly pattern with

548　　　　　westerly anomalies in the troposphere, easterly anomalies at 20-70 hPa and westerly

549　　　　　anomalies at 3-10 hPa. Despite its smaller amplitude in comparison to those obtained

550　　　　　from Austral winter and spring months, this well-structured wind anomaly pattern is

551　　　　　statistically significant all-year around. There is additional seasonal variation

552　　　　　superimposed on this annual average with noticeable upward movement during the

553　　　　　Boreal winter and spring and downward movement during the Austral late winter and

554　　　　　spring, consistent with the known annual cycle effect with stronger upwelling during

555　　　　　NH winter and weaker upwelling during SH winter.

556　　　3)　The tropical temperature response to P_{sw} is characterized by anomalous warming of 2

557　　　　　K at 30-50 hPa and up to 1 K near the tropopause during the Boreal winter and spring

558   accompanied by up to 0.5 K cooling in the troposphere during the Austral winter and

559   spring. There is an anomalous downward propagation of positive temperature

560   anomalies from the upper stratosphere to the lower stratosphere over a period of a

561   year starting from December. The combined effect may cause a systematic

562   modulation of the annual cycle in the tropical stratospheric temperature and wind.

563   It remains to be understood what mechanism can cause the observed seasonal

564 modulation of the annual cycle by solar wind dynamic pressure leading to statistically

565 significant changes of the QBO. As the annual cycle in tropical temperature and zonal

566 wind is strongly coupled to the annual cycle in stratospheric water vapour, ozone and

567 wave activity from the troposphere [*Mote et al*., 1995; *Fueglistaler et al*., 2009], a next

568 step would be to look for changes in convective water vapour, ozone and/or upward

569 propagating equatorial waves. Through such related research, the pathways by which the

570 effect of solar wind variability, which is observable mainly in the lower thermosphere and

571 above, may propagate to the lower atmosphere can be better understood.

572

578

579

References

581   Arnold, N. F., and T. R. Robinson (2001), Solar magnetic flux influences on the dynamics of the winter middle

582   atmosphere, *Geophys. Res. Lett.*, *28*(12), 2381-2384.

583   Baldwin, M. P., and L. J. Gray (2005), Tropical stratospheric zonal winds in ECMWF ERA-40 reanalysis,

584   rocketsonde data, and rawinsonde data, *Geophys. Res. Lett.*, *32*(9), art. no.-L09806.

585   Baldwin, M. P., et al. (2001), The quasi-biennial oscillation, *Reviews of Geophysics*, *39*(2), 179-229.

586   Christiansen, B. (2010), Stratospheric bimodality: Can the equatorial QBO explain the regime behavior of the

587   NH winter vortex?, *J. Clim.*, *23*, 3953-3966.

588   Cordero, E. C., and T. R. Nathan (2005), A new pathway for communicating the 11-year solar cycle signal to

589   the QBO, *Geophys. Res. Lett.*, *32*, L18805, doi:18810.11029/12005GL023696.

590   Crooks, S. A., and L. J. Gray (2005), Characterization of the 11-year solar signal using a multiple regression

591   analysis of the ERA-40 dataset, *J. Clim.*, *18*(7), 996-1015.

592   de Artigasa, M. Z., and A. Elias (2005), The equatorial stratospheric QBO and geomagnetic activity, *J. Atmos.*

593   *Sol.-Terr. Phys.*, *67*, 1280–1286.

594   Dunkerton, T. J. (1983), Modification of stratospheric circulation by race constituent changes?, *J. Geophys.*

595   *Res.*, *88*, 10 831–810 836.

596   Dunkerton, T. J. (1990), Annual variation of deseasonalized mean flow acceleration the the equatorial lower

597   stratosphere, *J. Meteor. Soc. Japan*, *68*, 499-508.

598   Dunkerton, T. J. (1991), Nonlinear propagation of zonal winds in an atmosphere with Newtonian cooling and

599   equatorial wavedriving, *J. Atmos. Sci.*, *48*, 236–263.

600   Dunkerton, T. J. (2000), Inferences about QBO dynamics from the atmospheric ''Tape Recorder'' effect, *J.*

601   *Atmos. Sci.*, *57*, 230-245.

602   Dunkerton, T. J., and D. P. Delisi (1997), Interaction of the quasi-biennial oscillation and stratopause

603   semiannual oscillation, *J. Geophys. Res.*, *102*(D22), 26,107–26.

604   Fischer, P., and K. K. Tung (2008), A reexamination of the QBO period modulation by the solar cycle, *J.*

605   *Geophys. Res.*, *113*, D07114, doi:07110.01029/02007JD008983.

606   Fueglistaler, S., A. E. Dessler, T. J. Dunkerton, I. Folkins, Q. Fu, and P. W. Mote (2009), Tropical tropopause

607   layer, *Rev. Geophys.*, *47*, RG1004, doi:1010.1029/2008RG000267.

608 Gray, L. J., et al. (2010), Solar influence on climate, *Rev. Geophys.*, doi:10.1029/2009RG000282.

609 Gray, L. J., S. J. Phipps, T. J. Dunkerton, M. P. Baldwin, E. F. Drysdale, and M. R. Allen (2001), A data study

610   of the influence of the equatorial upper stratosphere on northern-hemisphere stratospheric sudden

611   warmings, *Q. J. R. Meteorol. Soc.*, *127*(576), 1985-2003.

612 Haigh, J. D. (2003), The effects of solar variability on the Earth's climate, *Philos. Trans. R. Soc. Lond. Ser. A-*

613   *Math. Phys. Eng. Sci.*, *361*(1802), 95-111.

614 Hamilton, K. (2002), A note on the quasi-decadal modulation of the stratospheric QBO period, *J. Clim.*, *15*,

615   2562-2565.

616 Hampson, J., and P. Haynes (2004), Phase alignment of the tropical stratospheric QBO in the annual cycle. *J.*

617   *Atmos. Sci.*, *61*, 2627–2637.

618 Holton, J. R., and R. S. Lindzen (1972), An updated theory for the quasi biennial oscillation of the tropical

619   stratosphere, *J. Atmos. Sci.*, *29*, 1076-1080.

620 Holton, J. R., P. H. Haynes, M. E. Mcintyre, A. R. Douglass, R. B. Rood, and L. Pfister (1995), Stratosphere-

621   troposphere exchange, *Reviews of Geophysics*, *33*, 403-439.

622 Hood, L. L. (2004), Effects of solar UV variability on the stratosphere, in *Solar variability and its effect on the*

623   *Earth.s atmosphere and climate system*, edited by J. Pap, P. Fox, C. Frolich, H. Hudson, J. Kuhn, J.

624   McCormack, G. R. North, W. Sprigg and S. Wu, AGU Monograph Series, Washington D.C.

625 Jarvis, M. J. (1996), Quasi-Biennial Oscillation effects in the semidiurnal tide of the Antarctic lower

626   thermosphere, *Geophys. Res. Lett.*, 23(19), 2661–2664, doi:10.1029/96GL02394.

627 Kane, R. P. (2005), Differences in the quasi-biennial oscillation and quasi-triennial oscillation characteristics of

628   the solar, interplanetary, and terrestrial parameters, *J. Geophys. Res.*, *110*, A01108,

629   doi:01110.01029/02004JA010606.

630 King, J. H., and N. E. Papitashvili (2005), Solar wind spatial scales in and comparisons of hourly Wind and

631   ACE plasma and magnetic field data, *J. Geophys. Res.*, *110*, A02104, doi:02110.01029/02004JA010649.

632 Kinnersley, J. S., and S. Pawson (1996), The descent rates of the shear zones of the equatorial QBO, *J. Atmos.*

633   *Sci.*, *53*, 1937–1949.

634 Kodera, K., and Y. Kuroda (2002), Dynamical response to the solar cycle, *J. Geophys. Res.*, *107*(D24), D4749,

635   doi:4710.1029/2002JD002224.

636 Kuai, L., R.-L. Shia, X. Jiang, K. K. Tung, and Y. L. Yung (2009a), Modulation of the period of the Quasi-

637   Biennial Oscillation by the solar cycle, *J. Atmos. Sci.*, *66*(8), 2418-2428.

638   Kuai, L., R. L. Shia, X. Jiang, K. K. Tung, and Y. L. Yung (2009b), Nonstationary Synchronization of

639   Equatorial QBO with SAO in Observations and a Model, *J. Atmos. Sci.*, *66*, 1654–1664.

640   Labitzke, K., M. Kunze, and S. Bronnimann (2006), Sunspots, the QBO and the stratosphere in the North Polar

641   Region - 20 years later, *Meteorol. Zeitschrift*, *15*, 355-363.

642   Langematz, U., J. L. Grenfell, K. Matthes, P. Mieth, M. Kunze, B. Steil, and C. Brühl (2005), Chemical effects

643   in 11-year solar cycle simulations with the Freie Universität Berlin Climate Middle Atmosphere Model

644   with online chemistry (FUB-CMAM-CHEM), *Geophys. Res. Lett.*, *32*, L13803,

645   doi:13810.11029/12005GL022686.

646   Lockwood, M., Bell, C., T. Woollings, R. G. Harrison, L. J. Gray, and J. D. Haigh (2010a), Top-down solar

647   modulation of climate: Evidence for centennial-scale change, *Environ. Res. Lett.*, *5*, 034008,

648   doi:034010.031088/031748-039326/034005/034003/034008.

649   Lockwood, M., R. G. Harrison, T. Woollings, S. K. Solanki (2010b), Are cold winters in Europe associated

650   with low solar activity? *Environ. Res. Lett. 5,* 024001.

651   Lu , B. W., L. Pandolfo, K. Hamilton (2009), Nonlinear representation of the quasi-biennial oscillation. *J Atmos*

652   *Sci.*, *66*, 1886–1904.

653   Lu, H., M. J. Jarvis, and R. E. Hibbins (2008a), Possible solar wind effect on the Northern Annular Mode and

654   northern hemispheric circulation during winter and spring, *J. Geophys. Res.*, *113*, D23104,

655   doi:23110.21029/12008JD010848.

656   Lu, H., M. A. Clilverd, A. Seppälä, and L. L. Hood (2008b), Geomagnetic perturbations on stratospheric

657   circulation in late winter and spring, *J. Geophys. Res.*, *113*, D16106, doi:16110.11029/12007JD008915.

658   Lu, H., M. J. Jarvis, H. F. Graf, P. C. Young, and R. B. Horne (2007), Atmospheric temperature response to

659   solar irradiance and geomagnetic activity, *J. Geophys. Res.*, *112*, D11109,

660   doi:11110.11029/12006JD007864.

661   Mayr, H. G., J. G. Mengel, and C. L. Wolff (2005), Wave-driven equatorial annual oscillation induced and

662   modulated by the solar cycle, *Geophys. Res. Lett.*, *32*, L20811, doi:20810.21029/22005GL023090.

663   Mayr, H. G., J. G. Mengel, C. L. Wolff, and H. S. Porter (2006), QBO as potential amplifier of solar cycle

664   influence, *Geophys. Res. Lett.*, *33*, L05812, doi:05810.01029/02005GL025650.

665   McCormack, J. P. (2003), The influence of the 11-year solar cycle on the quasi-biennial oscillation, *Geophys.*

666   *Res. Lett.,* *30*(22), 2162, doi:2110.1029/2003GL018314.

667   McCormack, J. P., D. E. Siskind, and L. L. Hood (2007), Solar-QBO interaction and its impact on stratospheric

668   ozone in a zonally averaged photochemical transport model of the middle atmosphere, *J. Geophys. Res.*,

669   *112*, D16109, doi:16110.11029/12006JD008369.

670   Mote, P. W., K. H. Rosenlof, J. R. Holton, R. S. Harwood, and J. W. Waters (1995), Seasonal-Variations of

671   Water-Vapor in the Tropical Lower Stratosphere, *Geophys. Res. Lett.*, *22*(9), 1093-1096.

672   Nathan, T. R., and E. C. Cordero (2007), An ozone-modified refractive index for vertically propagating

673   planetary waves, *J. Geophys. Res.*, *112*, D02105, doi:02110.01029/02006JD007357.

674   Naujokat, B. (1986), An update of the observed quasi-biennial oscillation of the stratospheric winds over the

675   tropics., *J. Atmos. Sci.*, *43*, 1873-1877.

676   Norton, W. A. (2006), Tropical wave driving of the annual cycle in tropical tropopause temperatures. Part II:

677   Model results, *J. Atmos. Sci.*, *63*, 1420–1431.

678   Palmer, M. A., and L. J. Gray (2005), Modeling the atmospheric response to solar irradiance changes using a

679   GCM with a realistic QBO, *Geophys. Res. Lett.*, *32*(24).

680   Pascoe, C. L., L. J. Gray, S. A. Crooks, M. N. Juckes, and M. P. Baldwin (2005), The quasi-biennial oscillation:

681   Analysis using ERA-40 data, *J. Geophys. Res.*, *110*(D8), D08105, doi:08110.01029/02004JD004941.

682   Plumb, R. A., and R. C. Bell (1982), A model of the quasi-biennial oscillation on an equatorial beta-plane, *Q. J.*

683   *R. Meteorol. Soc.*, *108*, 335-352.

684   Punge, H. J., and M. A. Giorgetta (2007), Differences between the QBO in the first and in the second half of the

685   ERA-40 reanalysis, *Atmos. Chem. Phys.*, 7, 599–608.

686   Randall, C.E., V.L. Harvey, G.L. Manney, Y. Orsolini, M. Codrescu, C. Sioris, S. Brohede, C.S. Haley, L.L.

687   Gordley, J.M. Zawodny, and J.M. Russell (2005), Stratospheric effects of energetic particle precipitation

688   in 2003-2004, *Geophys. Res. Lett.*, *32* (5), L05802, doi:10.1029/2004GL022003.

689   Randall, C.E., V.L. Harvey, C.S. Singleton, S.M. Bailey, P.F. Bernath, M. Codrescu, H. Nakajima, and J.M.

690   Russell III (2007), Energetic particle precipitation effects on the Southern Hemisphere stratosphere in

691   1992–2005, , *J. Geophys. Res.*, *112*, D08308, doi:10.1029/2006JD007696.

692   Randall, C.E., V.L. Harvey, C.S. Singleton, P.F. Bernath, C.D. Boone, and J.U. Kozyra (2006), Enhanced NO_x

693   in 2006 linked to strong upper stratospheric Arctic vortex, *Geophys. Res. Lett.*, *33*, L18811,

694   doi:10.1029/2006GL027160.

695   Randel, W. J., R. R. Garcia, N. Calvo, and D. Marsh (2009), ENSO influence on zonal mean temperature and

696   ozone in the tropical lower stratosphere, *Geophys. Res. Lett.*, 36, L15822, doi:10.1029/2009GL039343.

697   Randel, W. J., F. Wu, J. M. Russel III, A. Roche, J. W. Waters (1998), Seasonal cycles and QBO variations in

698   stratospheric CH_4 and H_2O observed in UARS HALOE data, *J. Atmos. Sci.*, *55*, 163-185.

699   Randel, W. J., F. Wu, S. J. Oltmans, K. H. Rosenlof, and G. E. Nedoluha (2004), Interannual changes of

700   stratospheric water vapor and correlations with tropical tropopause temperatures, *J. Atmos. Sci.*, *61*, 2133–

701   2148.

702   Rosenlof, K. H. (1995), Seasonal cycle of the residual mean meridional circulation in the stratosphere, *J.*

703   *Geophys. Res.*, *100*(D3), 5173–5191, doi:5110.1029/5194JD03122.

704   Rozanov, E., L. Callis, M. Schlesinger, F. Yang, N. Andronova, and V. Zubov (2005), Atmospheric response to

705   NO_y source due to energetic electron precipitation, *Geophys. Res. Lett.*, *32*(14), L14811,

706   doi:10.1029/2005GL023041.

707   Salby, M., and P. Callaghan (2000), Connection between the solar cycle and the QBO: The missing link, *J.*

708   *Clim.*, *13*(14), 2652-2662.

709   Seppälä, A., C. E. Randall, M. A. Clilverd, E. Rozanov, and C. J. Rodger (2009), Geomagnetic activity and

710   polar surface air temperature variability, *J. Geophys. Res.*, 114, A10312, doi:10.1029/2008JA014029.

711   Seppälä, A., P.T. Verronen, M.A. Clilverd, C.E. Randall, J. Tamminen, V. Sofieva, L. Backman, and E. Kyrölä

712   (2007), Arctic and Antarctic polar winter NO_X and energetic particle precipitation in 2002-2006, *Geophys.*

713   *Res. Lett.*, *34*, L12810, doi:10.1029/2007GL029733.

714   Siskind, D.E., S.D. Eckermann, L. Coy, J.P. McCormack, and C.E. Randall (2007), On recent interannual

715   variability of the Arctic winter mesosphere: Implications for tracer descent, *Geophys. Res. Lett.*, *34*,

716   L09806, doi:10.1029/2007GL029293.

717   Solomon, S., P.J. Crutzen, and R.G. Roble, Photochemical coupling between the thermosphere and the lower

718   atmosphere: 1. Odd nitrogen from 50 to 120 km, *J. Geophys. Res.*, *87*, 7206-7220, 1982.

719   Soukharev, B. E., and L. L. Hood (2001), Possible solar modulation of the equatorial quasi-biennial oscillation:

720   Additional statistical evidence, *J. Geophys. Res.*, *106*(D14), 14855-14868.

721   Sugiura, M., and D. J. Poros (1977), Solar-Generated Quasi-Biennial Geomagnetic Variation, *J. geophys. Res.*,

722   *82*, 5621–5628.

723   Taguchi, M. (2009), Wave driving in the tropical lower stratosphere as simulated by WACCM. Part I: Annual

724   cycle, *J. Atmos. Sci.*, *66*, 2029–2043.

725   Uppala, S. M., et al. (2005), The ERA-40 reanalysis, *Q. J. R. Meteorol. Soc.*, *131*(612), 2961-3012.

726   Wang, M., J. E. Overland, D. B. Percival, and H. O. Mofjeld (2006), Change in the Arctic influence on Bering

727   Sea climate during the twentieth century, *Int J Climatol*, *26*(4), 531-539.

728   Woollings, T., M. Lockwood, G. Masato, C. Bell, and L. Gray (2010), Enhanced signature of solar variability in

729   Eurasian winter climate, *Geophys. Res. Lett.*, *37*, L20805, doi:20810.21029/22010GL044601.

730   Yulaeva, E., J. R. Holton, and J. M. Wallace (1994), On the cause of the annual cycle in tropical lower

731   stratospheric temperature, *J. Atmos. Sci.*, *51*, 169-174.

732

734   **Figure 1**. Height-time cross section of the monthly-mean zonal wind (top two panels) and the

735   QBO time series (*i.e.* de-seasonalized monthly mean zonal mean zonal wind averaged over

736   5°S-5°N) (bottom two panels) for the period of 1958-2009. Red and blue colors represent

737   westerly and easterly winds respectively.

738   **Figure 2**. Time series of monthly solar wind dynamic pressure P_{sw} (blue line), with its high &

739   low frequency components shown as the red and dark solid black lines. The frequency

740   separation is done by treating the original monthly P_{sw} with an order 11 Butterworth high-

741   pass filter with a cut-off period of 36 months.

742   **Figure 3.** The QBO phase occurrences under HP (1st row), and under LP (2nd row) at 70-30

743   hPa pressure levels (from left to right), calculated based on daily data. Westerly winds

744   (wQBO) are donated as solid lines and easterly winds (eQBO) are donated as gray shaded

745   and dashed contour lines. wQBO and eQBO are defined as > 0.25 and < -0.25 of the

746   normalized monthly mean of the QBO.

747   **Figure 4.** The QBO phase occurrences in relation to high (HP, solid line with +) and low

748   (LP, dashed line with o) solar wind dynamic pressure for eQBO (1st row), under wQBO (2nd

749   row) phases at 70-30 hPa pressure levels (from left to right). HP and LP are defined as $>$

750   0.25 and < -0.25 of the normalized monthly P_{sw} median.

751   **Figure 5**. (a) Vertical profile of the annual mean tropical wind (solid line) and ± one standard

752   deviation (dotted lines); (b) Departure from the annual mean for HP and LP conditions (solid

753   lines) for the period of 1963-2009; (c) same as (b) but based on data from 1979-2009; (d)

754   same as (b) but based on data when two years after each major volcanic eruption are

755   excluded. In (b), (c) and (d), 95% confidence intervals are shown as dotted lines for both HP

756   and LP conditions. When the dotted lines do not overlap, it indicates that the average

757   differences between the HP and LP groups are significant at or above the 95% confidence

758   level. All the departures are calculated as deviations from the monthly mean based on daily

759   data which is then aggregated to give the annual mean departure.

760   **Figure 6.** Same as figure 5b but for December-February (a), March-May (b), June-August

761   (c), and September-November (d) means. The departures from the seasonal means are

762   calculated based on daily data aggregated into a seasonal mean departure. The usage of the

763   lines and the definition of significant levels are the same as figure 5.

764   **Figure 7.** Height-time cross section of running composite difference of the daily equatorial

765   zonal wind (in m s^{-1}) from 1st of June to 30th of October for HP-LP condition. A 31-day

766   running window is applied to both the wind and P_{sw} without any time lag. (a): the linear

767   regression is based on raw P_{sw}. (b): A high-pass filter with cut-off period of 1095-day (~3-

768   years). (c): same as (b) but data affected by the major volcanic eruptions are excluded. (d):

769   same as (b) but data affected by the major El Niño (1972, 1973, 1982, 1983, 1997, and 1998)

770   are excluded.

771   **Figure 8.** Correlations between the July to October averaged high frequency P_{sw} (*i.e.* with

772   period shorter than 3 years, denoted as $P_{sw\ JASO}$) and the averaged QBO for the same calendar

773   months (denoted as QBO$_{JASO}$) at 50 hPa (a) and 30 hPa (b), respectively. Individual years are

774   shown as two digital numbers. Years affected by major volcanic eruptions and major El Niño

775   events are highlighted as red and green squares. The correlation coefficient, statistical

776   confidence level (in brackets), and number of samples used are given in the top of the panels

777   (also in brackets).

778   **Figure 9.** Same as Figure 7(a), except that the equatorial zonal-mean zonal wind is replaced

779   by equatorial zonal-mean temperature and the x-axis are extended from 1st of the January to

780   31st of the December and y-axis from 1000 hPa to 1 hPa.

781 **Figure 10**. (a) Vertical profile of tropical (5°S-5°N) climatological mean annual pattern of

782 zonal-mean zonal wind in m s^{-1}. Westerly winds are donated as solid lines and easterly winds

783 are donated as gray shaded and dashed contour lines. (b) Vertical profile of tropical

784 climatological mean annual variation of temperature (thick black lines, lower panel) and

785 temperature anomalies from annual mean profile (shaded contour) in K. Negative

786 temperature anomalies are donated with gray shading.

787 **Figure 11**. Histograms of the QBO phase transitions (zero crossings based on daily data) at

788 10hPa, 20hPa, 30hPa, 50hPa and 70hPa (top to bottom) grouped by month. Westerly to

789 easterly transitions are displayed in the left-hand panels, while easterly to westerly transitions

790 are shown in the right-hand panels. The climatology and variability faster than 6 months were

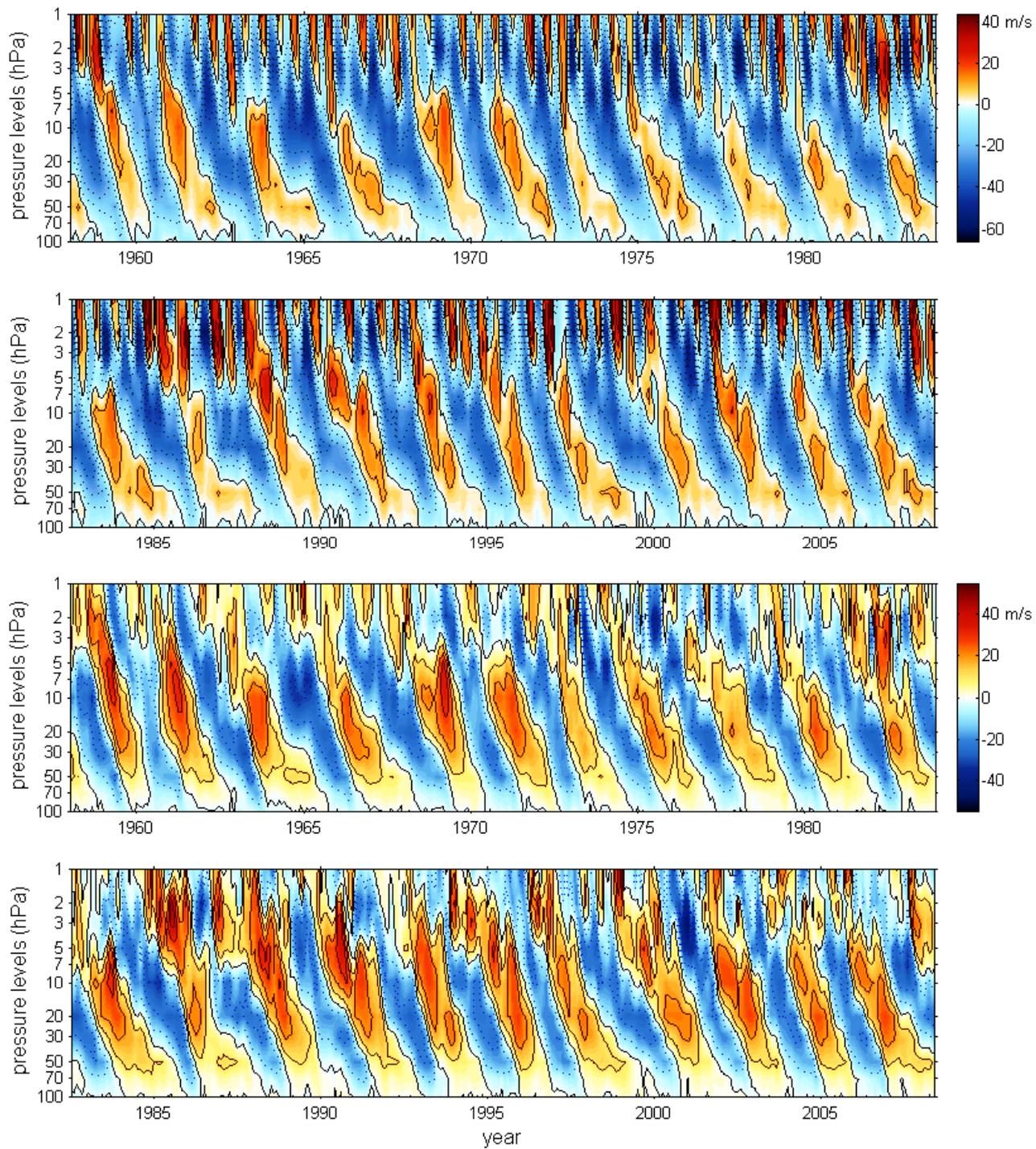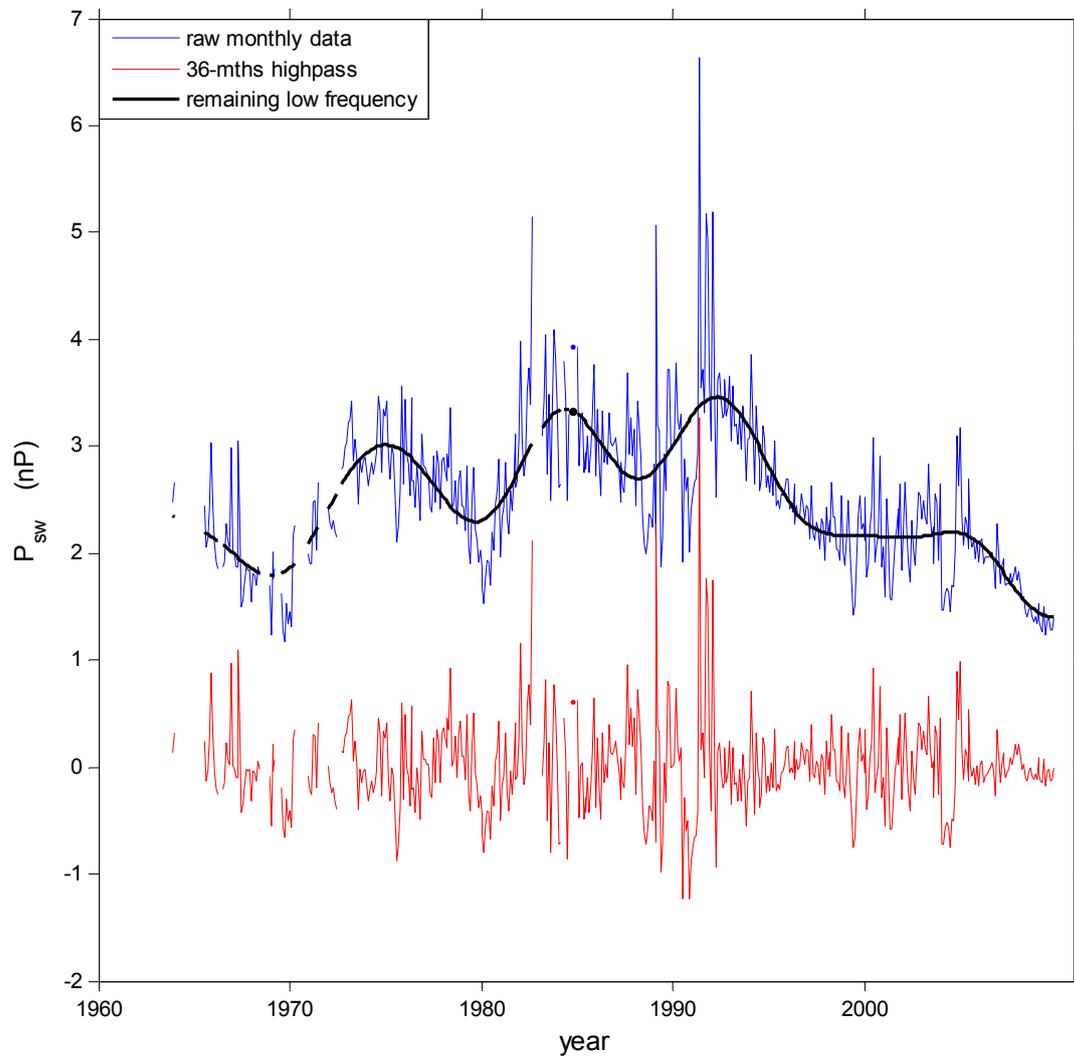791 removed before the transitions were determined. The years of the transitions are donated by
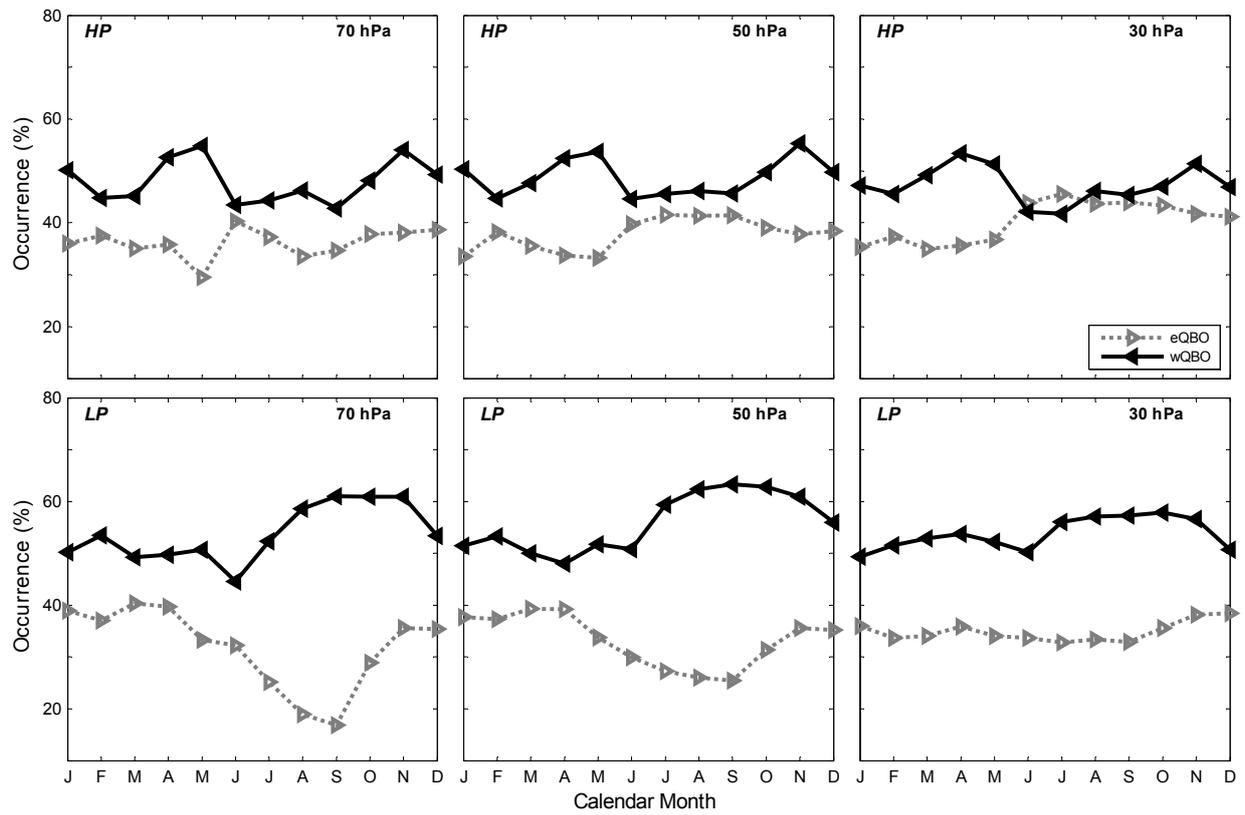
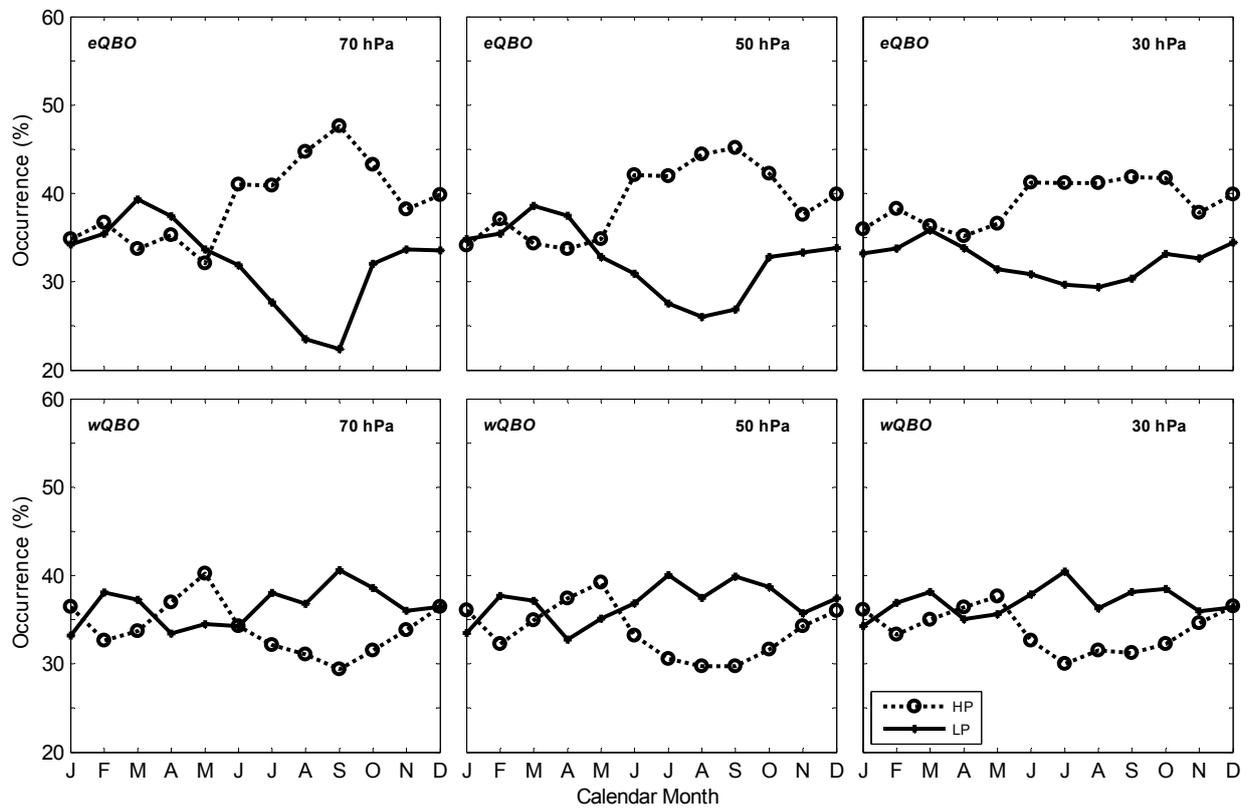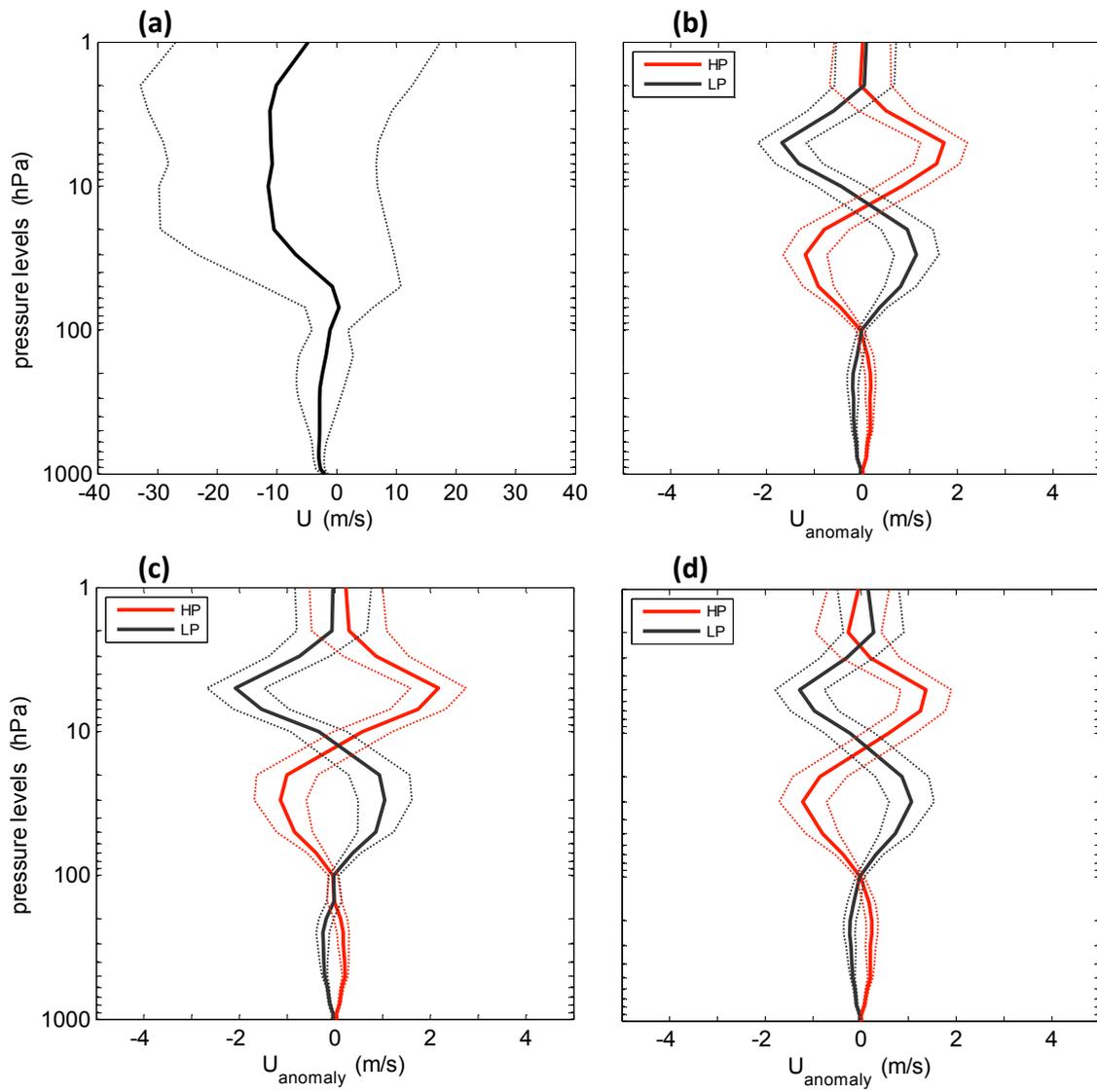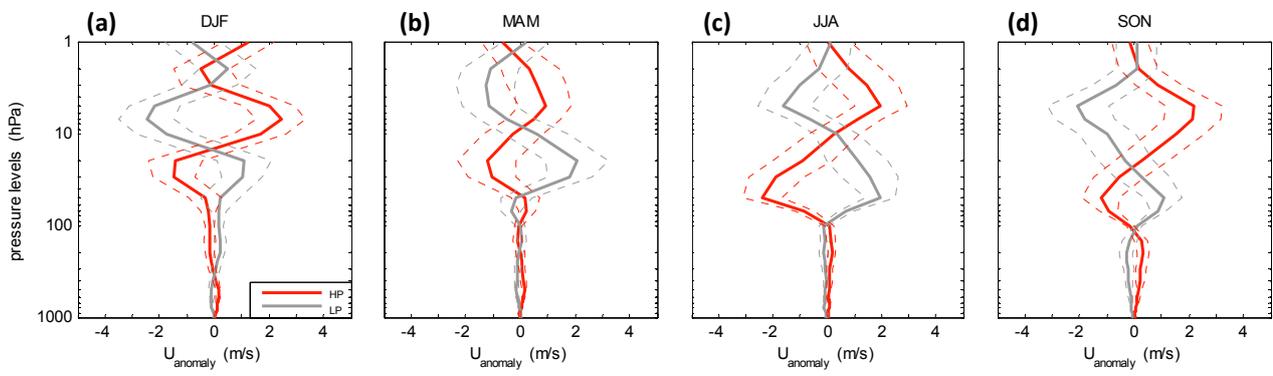792 two digital numbers.

Figure 1

Figure 2

Figure 3

Figure 4

Figure 5

Figure 6

(a)

(b)

(c)

(d)
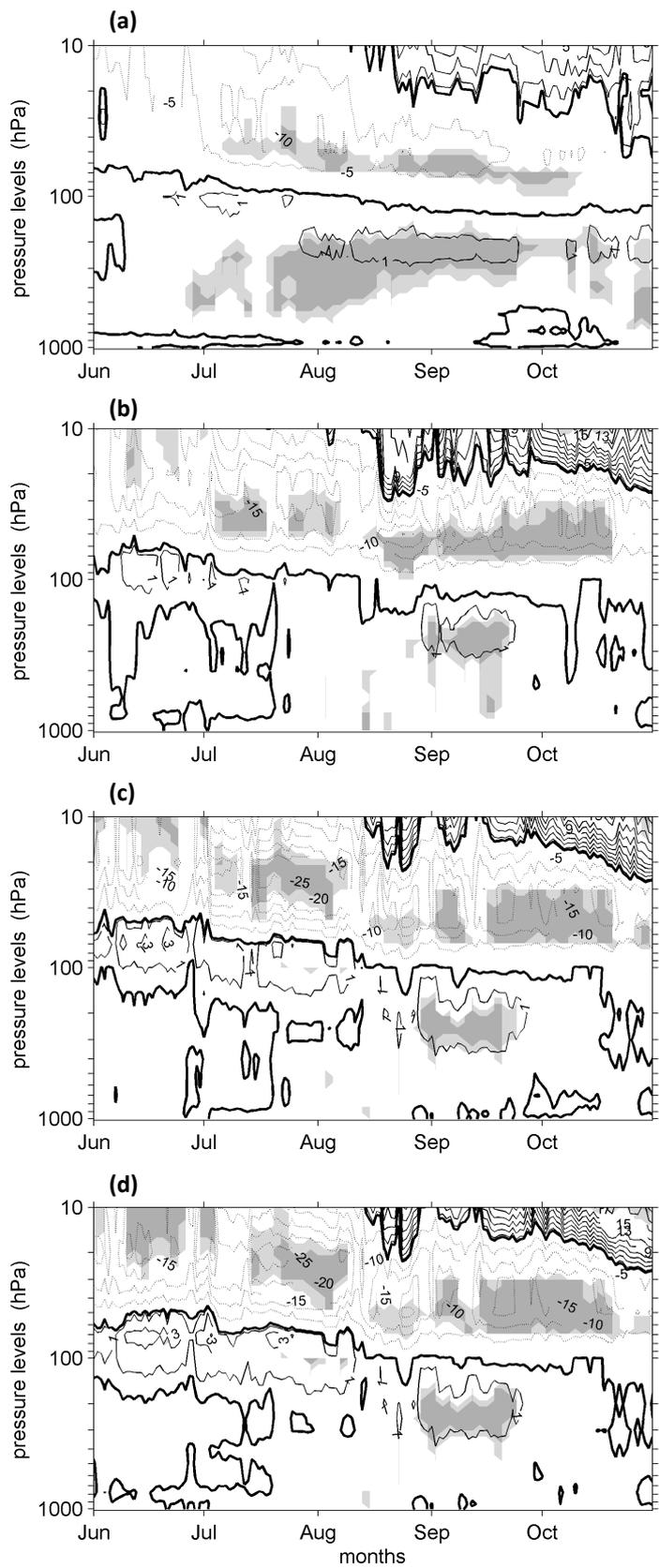
Figure 7

Figure 8

Figure 9

Figure 10

Figure 11

```
        Westerly->Easterly                    Easterly->Westerly
10 hPa                    06
                          04
                          90                    03
                          80                    98              00
                       85 75                    94              81
                 02    69 61                    84 07     05    76
        88    95 99    08 66 59                 68 96 70 79 91 72 62
  64    83 93 78 73    97 57 55           87    54 89 56 74 60 65 58
  J  F  M  A  M  J  J  A  S  O  N  D       J  F  M  A  M  J  J  A  S  O  N  D

20 hPa                                                             07
                          06                                      05
           83          04 97                          03       89
        09    67       02 85                       96 98       79
        86 91 64 93       95 99 61     86 75       92 87 01 68 84 96 72
  58 60 72 88 53 76    78 73 69 55     66 59       63 82 77 54 60 70 56
  J  F  M  A  M  J  J  A  S  O  N  D       J  F  M  A  M  J  J  A  S  O  N  D

30 hPa                                 04
                                       97
        07    00                       80 08          92
        74 05    91 09          88     73 90          87
  03 65 79 62 81 86 83          69     71 69    75    82          01 98
  98 56 60 58 72 67 76    93 95 53     57 61 06 66 59    63    77 94 54 84
  J  F  M  A  M  J  J  A  S  O  N  D       J  F  M  A  M  J  J  A  S  O  N  D

50 hPa              07
                    03
           98 05 91                       08 90
           96 70 89                       06 80
           94 65 79                    02 04 97 69
        01 84 60 74 62                 99 85 71 66 75       87
  77 87 68 54 56 72 58          81     95 78 55 73 61 57 59    63 82    92
  J  F  M  A  M  J  J  A  S  O  N  D       J  F  M  A  M  J  J  A  S  O  N  D

70 hPa           98    05
                 96    79
                 84 01 74                          07       75
        92       78 73 71 07 08           99 06 85       66
        82 87    70 72 65 89 03     93    95 97 78 90    59 87 91
  63    77 68 94 60 56 54 58 91     09 55 53 73 69 71 80 61 57 63 82
  J  F  M  A  M  J  J  A  S  O  N  D       J  F  M  A  M  J  J  A  S  O  N  D
```